0026-895X/07/7203-545–552$20.00
MOLECULAR PHARMACOLOGY
Copyright © 2007 The American Society for Pharmacology and Experimental Therapeutics
Mol Pharmacol 72:545–552, 2007

Vol. 72, No. 3
36350/3245089
Printed in U.S.A.

Philinopside E, a New Sulfated Saponin from Sea Cucumber, Blocks the Interaction between Kinase Insert Domain-Containing Receptor (KDR) and $\alpha_v\beta_3$ Integrin via Binding to the Extracellular Domain of KDR

Fang Tian, Cai-hua Zhu, Xiong-wen Zhang, Xin Xie, Xian-liang Xin, Yang-hua Yi, Li-ping Lin, Mei-yu Geng, and Jian Ding

Division of Antitumor Pharmacology, State Key Laboratory of Drug Research (F.T., C.Z., X.Z., L.L., M.G., J.D.), National Center for Drug Screening (X.X.), Shanghai Institute of Materia Medica, Chinese Academy of Sciences, Shanghai, People's Republic of China; Department of Pharmacology and Glycobiology, Marine Drug and Food Institute, Ocean University of China, Qingdao, People's Republic of China (X.X., M.G.); and Research Center for Marine Drugs, School of Pharmacy, Second Military Medical University, Shanghai, People's Republic of China (Y.Y.)

Received March 26, 2007; accepted June 12, 2007

ABSTRACT

Vascular endothelial growth factor (VEGF) signaling pathway is essential for tumor angiogenesis and has long been recognized as a promising target for cancer therapy. Current view holds that physical interaction between $\alpha_v\beta_3$ integrin and kinase insert domain-containing receptor (KDR) is important in regulating angiogenesis and tumor development. We have reported previously that a new marine-derived compound, philinopside E (PE), exhibited the antiangiogenic activity via inhibition on KDR phosphorylation and downstream signaling. Herein, we have further demonstrated that PE specifically interacts with KDR extracellular domain, which is distinct from conventional small-molecule inhibitors targeting cytoplasmic kinase domain, to block its interaction with VEGF and the downstream signaling. We also noted that PE markedly suppresses $\alpha_v\beta_3$ integrin-driven downstream signaling as a result of disturbance of the physical interaction between KDR and $\alpha_v\beta_3$ integrin in HMECs, followed by disruption of the actin cytoskeleton organization and decreased cell adhesion to vitronectin. All of these findings substantiate PE to be an unrecognized therapeutic class in tumor angiogenesis and, more importantly, help appeal the interest of the therapeutic potential in angiogenesis and cancer development via targeting integrin-KDR interaction in the future.

Angiogenesis, the process of sprouting of new capillaries from pre-existing blood vessels, is essential for sustained growth of solid tumor and metastasis. The overall process is regulated in malignant tissues by the balance of angiogenic stimuli and inhibitors (Ek et al., 2006). Among the various proangiogenic factors that have been identified, vascular endothelial growth factor and its cognate receptor vascular endothelial growth factor-2/KDR play a major role in tumor angiogenesis (Olsson et al., 2006). As being a member of the receptor tyrosine kinase (RTK) family, monomers of KDR become dimerized when binding with VEGF and autophosphorylate-specific tyrosine residues on the intracellular side of the receptor, then activate phospholipase Cγ-protein kinase C and phosphatidylinositol-3 kinase-Akt pathways, which contribute to the process of cell proliferation, migration, and vascularization (Holmqvist et al., 2004; Shibuya and Claesson-Welsh, 2006). Genetic and biochemical approaches have demonstrated the disruption of VEGF signaling via KDR inhibits tumor growth in animal models (Millauer et al., 1994; Saleh et al., 1996). In this context, VEGF-KDR signaling pathway has long been of great interest for drug discovery targeting tumor angiogenesis. Various approaches have been developed, including monoclonal antibodies against VEGF or KDR and small-molecule tyrosine kinase inhibitors of KDR (Jubb et al., 2006).

This work was supported by National Key Basic Research Project of China (grant 2004CB518903), National Natural Science Foundation (grant 30572201) and Knowledge Innovation Program of Chinese Academy of Sciences (grant KSCX2-YW-R-25).

F.T. and C.Z. contributed equally to this work.

Article, publication date, and citation information can be found at http://molpharm.aspetjournals.org.
doi:10.1124/mol.107.036350.

ABBREVIATIONS: PE, philinopside E; KDR, kinase insert domain-containing receptor; HMEC, human dermal microvascular endothelial cell; VEGF, vascular endothelial growth factor; RTK, receptor tyrosine kinase; ELISA, enzyme-linked-immunosorbent assay; SPR, surface plasmon resonance assay; FBS, fetal bovine serum; ERK, extracellular signal-regulated kinase; DMSO, dimethyl sulfoxide; PBS, phosphate-buffered saline; OPD, *o*-phenylenediamine dihydrochloride.

However, with the profound understanding of the roles of the complex nature of receptor tyrosine kinase-driven signal transduction pathways in angiogenesis, recent views hold that antiangiogenic agents might critically overlap in such a way that blockage of one pathway may lead to activation of compensatory pathways and inevitable tumor progression (Casanovas et al., 2005). It is becoming true that one pathway-targeted strategy is not currently encouraged when it is necessary to simultaneously block multiple signaling pathways (Kerbel, 2005).

Previous results from our group revealed that philinopside E, a new saponin compound derived from sea cucumber (Fig. 1), possessed dual antiangiogenesis and antitumor activity both in vitro and in vivo (Tian et al., 2005). PE induced endothelial cell apoptosis, followed by significant suppression on cell migration, cell adhesion, and tube formation of both human microvascular endothelial cells (HMECs) and human umbilical vein endothelial cells in a dose-dependent manner. In addition, PE showed marked growth inhibition in the mouse sarcoma 180 and hepatoma 22 models. Further immunofluorescent analysis indicated that PE reduced mouse sarcoma 180 tumor volumes by triggering apoptosis of both tumor and tumor-associated endothelial cells, preferentially targeting on human endothelial cells comparable with tumor cells. The preliminary underlying mechanism was elucidated to be attributed to its evident inhibition on KDR phosphorylation and subsequent downstream signaling (Tian et al., 2005). Recently, we noted that PE exhibited its favorable inhibition on integrin-KDR interaction. Given that KDR is capable of cooperating physically and functionally with integrins in regulation of angiogenesis and tumor development, we are thus encouraged to hypothesize that PE might have the potential to target the integrin-KDR interaction beyond a solely KDR-driven event.

The aim of the present study is to uncover the more detailed machineries involving antiangiogenic and antitumor activities of PE. With the availability of SPR-based binding analysis and coimmunoprecipitation evaluation, we found that PE specifically interacts with the extracellular domain of KDR and blocks $VEGF_{165}$ binding, followed by the sequential disturbance of the association between KDR and $\alpha_v\beta_3$ integrin, and thereby simultaneously suppressing both KDR-mediated and integrin-associated downstream signaling, accompanied by the disassembly of focal adhesion and reorganization of actin cytoskeleton. All of these findings further our understanding of the distinct roles of PE from the conventional ones and identify it as a new and hitherto unrecognized therapeutic class in angiogenesis and tumor development.

Materials and Methods

Materials and Cell Line. HMECs were cultured in MCDB131 containing 15% FBS, 1 ng/ml epidermal growth factor, and 1 mg/ml hydrocortisone. HMECs were maintained at 37°C under humidified 95%/5% in a mixture of air and CO_2. Antibodies against p-ERK, ERK, p-KDR, KDR, p-Akt, Akt, p-Rac1, Rac1, p-p21-activated kinase, p21-activated kinase, p-LIM kinase 1, and LIM kinase 1 were obtained from Cell Signaling Technology (Danvers, MA). Antibody against p-paxillin was obtained from BioSource International (Camarillo, CA). The anti-FAK and anti-paxillin antibodies were obtained from Santa Cruz Biotechnology (Santa Cruz, CA). Vitronectin, $\alpha_v\beta_3$ integrin, anti-$\alpha_v\beta_3$ integrin antibody, and anti-β_3 integrin antibody were purchased from Chemicon International (Temecula, CA). Alexa Fluor 532-phalloidin, Alexa Fluor 546/488-conjugated secondary antibodies, and the Prelong antifade kit were purchased from Invitrogen (Carlsbad, CA). Soluble KDR/Fc chimera, $VEGF_{165}$, anti-p-FAK antibody, cell culture medium MCDB131, endothelial cell growth supplement, 3-(4,5-dimethylthiazol-2-yl)-2,5-diphenyltetrazolium, heparin, OPD, and all other reagents were purchased from Sigma (St. Louis, MO).

Isolation and Purification of Philinopside E. Philinopside E was isolated from the sea cucumber *Pentacta quadrangularis* (collected near Guangdong Province, China, and identified by Professor J. R. Fang of Fujian Institute of Oceanic Research). The air-dried body walls (5 kg, dry weight) of *P. quadrangularis* were cut into pieces and extracted twice with refluxing ethanol. The combined extracts were evaporated in vacuo and further partitioned between water and chloroform. The water layer was extracted with *n*-butanol, and the organic layer was evaporated in vacuo to give the *n*-butanol extracts. The *n*-butanol extracts were concentrated, and the extracted residue was dissolved in water. Desalting was carried out by passing this fraction through a DA101 resin column (60 × 30 cm), first eluting the inorganic salts and polar impurities with water and then the crude glycoside fraction (8.1 g) with 80% ethanol. Then the fraction was separated by flash chromatography on silica gel (6/40 cm), $CHCl_3$/MeOH/H_2O 7.0:3.0:0.2, at 20 ml/min to yield the fraction containing PE along with other constituents. This faction was further separated by high-performance liquid chromatography (Zorbax 300 SB-C18, 9.4 mm × 25 cm, 55% MeOH/H_2O; flow rate, 1.5 ml/min) to afford the pure PE. The chemical structure of PE was determined by using ^1H and ^{13}C NMR spectrum, electrospray ionization-mass spectrometry, and IR spectrum assay and is shown in Fig. 1. The PE was dissolved in DMSO and diluted to desired concentra-

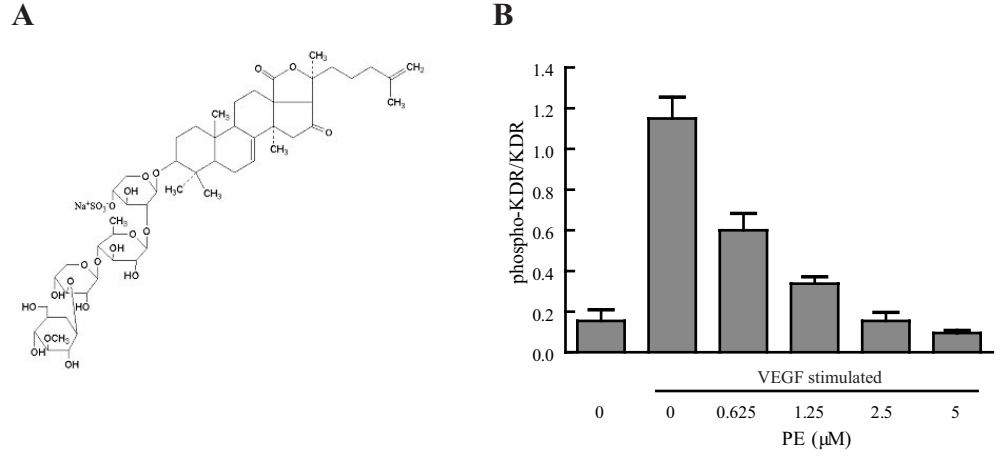

Fig. 1. PE inhibits $VEGF_{165}$-induced tyrosine phosphorylation of KDR in HMECs. A, the structure of philinopside E. B, starved HMECs were stimulated by 50 ng/ml $VEGF_{165}$ for 10 min. Cells were lysed, and lysates were incubated for 2 h in 96-well plates precoated with anti-KDR antibody. Phospho-KDR was detected by the addition of anti-phospho-KDR antibody for 1 h and then subjected to horseradish peroxidase-conjugated secondary antibody and 3,3′,5,5′-tetramethylbenzidine substrate. All of the experiments shown are representative of three independent experiments with similar results.

tions before use, with the concentration of DMSO kept lower than 0.1% in treated groups.

Western Blotting Analysis. Confluent HMECs were incubated for 24 h in MCDB131 containing 1% FBS, incubated for 1 h in MCDB131 without FBS in the presence PE or DMSO control, and then stimulated by the addition of VEGF (50 ng/ml) for 10 min. After stimulation, cells were lysed in lysis buffer (20 mM Tris-HCl, pH 8.0, 2 mM EDTA, 137 mM NaCl, 1 mM Na_3VO_4, 1 mM phenylmethylsulfonyl fluoride, 10% glycerol, and 1% Triton X-100). Lysates were clarified by centrifugation at 15,000*g* for 10 min, resolved by SDS-polyacrylamide gel electrophoresis, and transferred to polyvinylidene difluoride membranes. The membranes were blocked with 5% nonfat milk for 1 h at room temperature and then probed with primary antibody overnight at 4°C. Immunoreactive bands were visualized by incubation with horseradish peroxidase-conjugated secondary antibodies and application of an enhanced chemiluminescent system (GE Healthcare, Chalfont St. Giles, Buckinghamshire, UK). Each experiment was repeated at least three times, with representative blots presented.

Immunoprecipitation. HMECs were starved in MCDB131 with 1% fetal calf serum for 24 h. The cells were cultured on plates (for some studies, the plates were precoated with 2 μg/ml vitronectin) for 1 h and then treated for 1 h with various amount of PE and were stimulated with 50 ng/ml VEGF (for some studies) for 10 min at 37°C. The cells (approximately 5×10^6 per immunoprecipitation) were washed twice with ice-cold PBS and lysed at 4°C in 0.5 ml of lysis buffer containing 1% Nonidet P-40, 20 mM Tris-HCl, pH 7.4, 150 mM NaCl, 10% glycerol, 2 mM sodium vanadate, 1 mM phenylmethylsulfonyl fluoride, 10 mg/ml leupeptin, and 5 mg/ml aprotinin. Adherent material was removed from plates with a cell scraper, and the lysates were clarified by centrifugation at 15,000*g* for 10 min and precleared by incubation with protein A-agarose beads for 30 min at 4°C. After removal of albumin-agarose by brief centrifugation, the supernatants were transferred to fresh tubes for immunoprecipitation. Immunoprecipitations were routinely performed by incubating lysates with 1 mg/ml anti-KDR antibody as indicated for 3 h at 4°C. Immunocomplexes were collected by incubating lysates with protein A-agarose beads for a further 2 h. Immunoprecipitates were washed three times with lysis buffer, proteins were extracted with 2× SDS-polyacrylamide gel electrophoresis sample buffer, boiled for 10 min, and further analyzed by Western blotting.

Immunofluorescent Staining. HMECs were serum-starved using MCDB131 with 1% FBS for 24 h. Starved HMECs cultured on glass coverslips were stimulated with 20 ng/ml VEGF for 2 h, or the cells were cultured on glass coverslips precoated with vitronectin for 2 h (or with additional 20 ng/ml VEGF). In treatment groups, starved HMECs were plated in glass coverslips covered with vitronectin, and 50 ng/ml VEGF was added after incubation for 2 h and treatment with various concentrations of PE for an additional 1 h. After treatments, cells were washed three times with ice-cold PBS and then fixed in 4% paraformaldehyde in PBS for 30 min at 4°C. Cells were permeabilized with 0.1% Triton X-100 in PBS for 10 min at room temperature and then washed three times in PBS. Fixed and permeabilized cells were incubated with primary antibody for 1 h at room temperature, washed three times in PBS, and then incubated for 1 h at room temperature with secondary antibody conjugated to Alexa Fluor (Invitrogen). Cells were finally washed three times (5 min, each wash) in PBS. Coverslips were mounted onto microscope slides using ProLong antifade medium (Invitrogen). Filamentous actin was stained with Alexa Fluor 532-phalloidin in PBS (1 mg/ml) for 20 min at room temperature. Immunofluorescent staining was observed and photographed using a Leica laser scanning confocal microscope fitted with an objective lens set at ×100 (numerical aperture, 1.4, oil).

Surface Plasmon Resonance Assay. The kinetics and specificity of the binding reactions between PE and KDR/Fc chimera or $VEGF_{165}$ were carried out using the Biacore X SPR apparatus (Biacore/GE Healthcare). In brief, KDR/Fc chimera or $VEGF_{165}$ was immobilized on CM5 sensor chips, according to the protocol described in the Biacore X application handbook. The unreacted surface moieties were blocked with ethanolamine. To correct for nonspecific binding and bulk refractive index changes, a blank channel (FC2) without KDR/Fc chimera or $VEGF_{165}$ was used as a control for each experiment. Sensorgrams for all binding interactions were recorded in real time, and the blank channel readings were subtracted from the results before analysis. Changes in mass due to the binding response were recorded as resonance units. All binding experiments were performed at 25°C with a constant flow rate of 10 μl/min HBS-EP buffer (Biacore/GE Healthcare). The sensor chip surface was regenerated using 60 μl of 2 M NaCl in between experiments. For the determination of association and disassociation rate constants, the real-time binding capacity was recorded. For direct assessment of dissociation constants, the association phase was allowed to proceed to equilibrium. Binding kinetics and stoichiometry were determined by SPR using the Biacore software version 3.1.

ELISA Binding Assay. $VEGF_{165}$ (100 ng) in 100 μl of PBS was coated on ELISA plates overnight at 4°C. The wells were washed and blocked with 3% bovine serum albumin in PBS for 2 h. After 10 or 30 min of preincubation of KDR/Fc chimera (30 ng/ml) in PBS containing 10 μg/ml heparin, 0.2 mM $CaCl_2$, 1 mM $MgCl_2$, and 0.1% bovine serum albumin with or without various amount of PE, the mixture (100 μl) was added to each well. The binding was allowed to proceed at room temperature for 2 h. Then the wells were washed three times with PBS plus 0.05% Tween 20. The bound KDR/Fc chimera were determined by incubation with anti-KDR antibody for 1 h at room temperature and followed by anti-IgG-horseradish peroxidase and OPD substrate.

Cellular Tyrosine Kinase Assay. Confluent HMECs were incubated for 24 h in MCDB131 containing 1% FBS. Then the cells were incubated for 1 h with or without various amount of PE. KDR phosphorylation was stimulated by the addition of $VEGF_{165}$ for 10 min. Cells were washed with PBS and lysed with cell lysis buffer (20 mM Tris-HCl, pH 7.5, 150 mM NaCl, 1 mM Na_2EDTA, 1 mM EGTA, 1% Triton X-100, 2.5 mM sodium pyrophosphate, 1 mM β-glycerophosphate, 1 mM Na_3VO_4, and 1 μg/ml leupeptin). Lysates were transferred to 96-well plates precoated with anti-KDR antibody and incubated for 2 h. Phospho-KDR was detected by the addition of anti-phospho-KDR antibody for 1 h, and incubation with horseradish peroxidase-conjugated second antibodies was followed by 3,3′,5,5′-tetramethylbenzidine substrate.

Cell Adhesion Assay. HMECs were seeded into vitronectin coated 96-well plates at a density of 3×10^4 cells/well. After 30-min incubation, cells were fixed with prewarmed 4% formaldehyde in PBS and then permeabilized with 0.5% Triton-PBS solution. Cells were then stained with rhodamine-phalloidin for F-actin to outline the cytoplasm for cell area measurement and 4′,6-diamidino-2-phenylindole for nuclei detection. Images and data of the cells were obtained with an ArrayScan 4.0 HCS Reader (Cellomics, Pittsburgh, PA). A 10× microscope objective lens and appropriate filter sets were used for the imaging, and the Cell Spreading BioApplication was used to acquire and analyze the images after optimization of the application's protocol settings.

Statistics. The significance of differences between means was assessed by Student's *t* test. $P < 0.05$ was regarded as statistically significant.

Results

PE Inhibited $VEGF_{165}$-Induced Autophosphorylation of KDR in HMECs. Our previous studies have shown that PE could inhibit $VEGF_{165}$-induced phosphorylation of KDR. To further confirm this finding and get more detailed information, ELISA method was used to investigate the $VEGF_{165}$-induced autophosphorylation of KDR in HMECs upon the treatment of PE. Cells were preincubated with or

without PE for 1 h and then exposed to $VEGF_{165}$ for 10 min. The cells were then lysed with the lysates used for ELISA as described under *Materials and Methods*. As shown in Fig. 1, PE inhibited the phosphorylation of KDR induced by $VEGF_{165}$ in a dose-dependent manner with an IC_{50} value of 1.18 ± 0.68 μM.

PE Interacted with KDR Extracellular Domain but Not the Kinase Domain or VEGF Ligand and Blocked Its Association with $VEGF_{165}$. Because conventional small-molecule tyrosine kinase inhibitors are commonly identified to inhibit the catalytic activity of the kinase domain (Krause and Van Etten, 2005), we thus preferentially presumed that PE might inactivate KDR phosphorylation via its direct association with kinase domain. To answer this question, we first used a cell-free system containing the vascular endothelial growth factor receptor-2-CD (catalytic domain of KDR) as a soluble active kinase and substrates for phosphorylation (Zhong et al., 2005) to investigate whether PE is capable of inhibiting KDR phosphorylation activity. Contrary to our expectation, PE failed to inactivate the kinase activity of KDR even with the concentration of PE mounting to 100 μM (data not shown), indicating that PE is not a potential tyrosine kinase inhibitor targeting kinase domain as usual.

We next wondered whether PE might trigger the inactivation of tyrosine kinase via targeting VEGF or KDR extracellular domain. For this, we used the surface plasmon resonance technique to assess whether PE interacts with $VEGF_{165}$ or the extracellular domain of human KDR. With $VEGF_{165}$ or the KDR/Fc chimera (protein containing the amino acids residues of human KDR extracellular domain) immobilized on the CM5 sensor chip surface, different concentrations of PE were flowed over the chip surface. We found that PE was dose-dependently engaged with the extracellular domain of KDR/Fc chimera, yielding a K_d value of 10.7 μM (Fig. 2A and Table 1) but displayed no binding to $VEGF_{165}$ at the same concentration profiles (data not shown).

Because PE showed the ability to interact with KDR extracellular domain, this prompted us to hypothesize that it interrupts the association of KDR with $VEGF_{165}$. For this, we used an ELISA binding assay to examine the effect of PE on $VEGF_{165}$ binding to KDR/Fc chimera. We found that PE blocked the interaction of KDR/Fc chimera with $VEGF_{165}$ in a dose-dependent manner with an IC_{50} of 6.26 ± 2.43 μM. Preincubation of PE with KDR/Fc chimera for 30 min demonstrated a much more potent inhibition on this binding, yielding the IC_{50} value of 2.61 ± 0.86 μM (Fig. 2B).

PE Disrupted the Physical Interaction of KDR with $\alpha_v\beta_3$ Integrin in HMECs. Integrins physically collaborate with growth factor receptors to regulate a variety of biological processes. Increasing evidence has further demonstrated that the association of the αvβ3 integrin with KDR takes place outside of the cell through targeting the extracellular domain of β_3 subunit (Borges et al., 2000). Given that PE interacts with the extracellular domain of KDR, we thus presume that PE might interfere with the association of KDR with $\alpha_v\beta_3$ integrin. Here, both coimmunoprecipitation and immunoblotting analyses were used. HMECs were treated by exposing to VEGF or immobilized vitronectin, with cell lysates being immunoprecipitated by anti-KDR antibody. As shown in Fig. 3A, VEGF or vitronectin treatment caused a significant association between KDR and β_3 integrin, but no interaction was observed in starved and nontreated HMECs. It is noteworthy that this binding was dose-dependently disrupted by the treatment of PE (Fig. 3B). Next, we performed double-staining immunofluorescent assay. We found that KDR and $\alpha_v\beta_3$ integrin displayed an even distribution on

TABLE 1
Kinetic parameters of the interaction between PE and KDR
Data shown are typical of three independent experiments with similar results.

K_a (1/M · s)	K_d (1/s)	K_A (1/M)	K_D (M)
221	2.37×10^{-3}	9.32×10^{4}	1.07×10^{-5}

K_a, association rate constant; K_d, dissociation rate constant; K_A, equilibrium association constant; K_D, equilibrium dissociation constant.

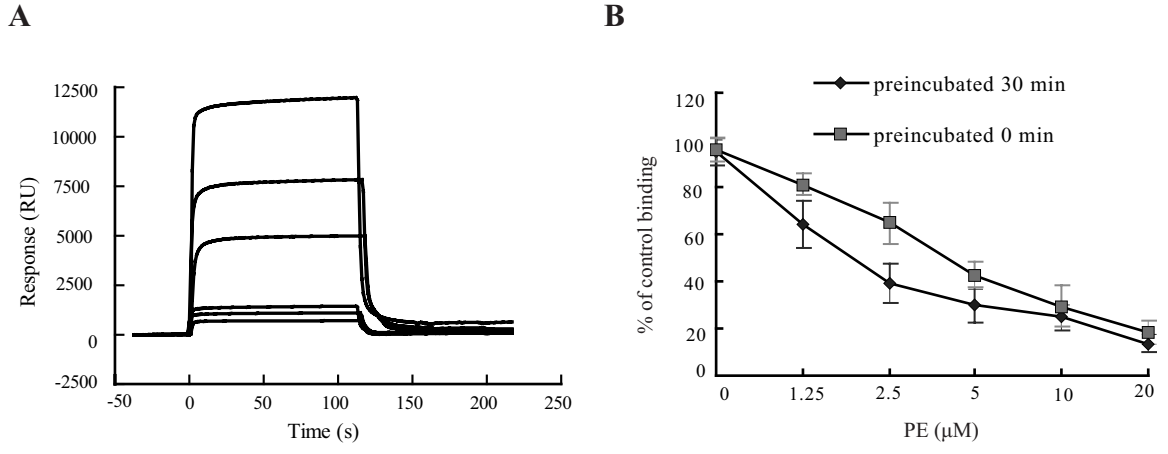

Fig. 2. PE binds to KDR extracellular domain and blocks the interaction between $VEGF_{165}$ and KDR. A, the interaction between PE and KDR/Fc chimera. PE at concentrations of 61.54, 30.77, 15.38, 7.69, 3.85, and 1.92 μM (from top to bottom) were injected over the KDR/Fc chimera immobilized surface, respectively, and binding profiles were recorded. SPR-based experiments were all performed at 25°C at a constant flow rate of 5 μl/min of HBS-EP buffer. Data shown are typical of three independent experiments with similar results. B, $VEGF_{165}$-coated ELISA plates were kept at 4°C overnight and then exposed to KDR/Fc chimera preincubated with or without PE for 0 or 30 min. The interaction was further allowed to proceed at room temperature for another 2 h. The bound KDR/Fc chimera was determined by incubation with anti-KDR antibody for 1 h at room temperature and was followed by the addition of anti-IgG-horseradish peroxidase and OPD substrate.

starved HMEC membranes (Fig. 3C). However, both $\alpha_v\beta_3$ integrin (the red staining) and KDR (the green staining) were clustered on the plasma membrane of the stimulated HMECs, indicating that both KDR and integrin were internalized upon the activation of VEGF. This cluster formation and internalization was significantly and dose-dependently abolished by the treatment with PE. All of these findings support that PE blocks the activation of KDR and subsequently KDR/integrin interaction.

PE Inhibited both KDR-Mediated and Integrin-Associated Downstream Signaling Stimulated by $VEGF_{165}$ and Vitronectin in HMECs. Physical and functional interactions between integrins and RTKs have been shown to be important signaling mechanisms during normal development and pathological processes in vascular biology (Eliceiri, 2001). In particular, the physical interaction between $\alpha_v\beta_3$ integrin and KDR is important for both of their downstream signaling (Soldi et al., 1999; Byzova et al., 2000). Because PE blocked the association between KDR and $\alpha_v\beta_3$ integrin, its effects on downstream components of KDR and $\alpha_v\beta_3$ integrin-linked signaling pathways were thus tested. $VEGF_{165}$ and vitronectin stimulated the activation of key molecules of both KDR and $\alpha_v\beta_3$ integrin signaling pathways. Treatment with 2.5 μM concentration of PE for 1 h showed significant inhibition on the KDR-driven p44 ERK phosphorylation and relatively mild inhibition on p42 ERK phosphorylation. In addition, PE significantly inhibited vitronectin-induced phosphorylation of FAK, paxillin and Akt, reflecting that PE is capable of inhibiting $\alpha_v\beta_3$ integrin-KDR association and thus the downstream signaling of $\alpha_v\beta_3$ integrin (Fig. 4).

PE Disassembled Focal Adhesion and Actin Cytoskeleton, Inactivated Rac, PAK1, and LIMK1 in HMECs, and Thus Suppressed Endothelial Cell Adhesion. Paxillin provides a platform for recruitment of many signaling proteins, including FAK, Src, and Abl. This protein complex organized by paxillin contributes to the organization of focal adhesion and actin cytoskeleton (Mitra et al., 2005). The aforementioned findings revealed that PE is capable of inactivating FAK; we thus intended to investigate whether PE exhibits inhibitory action on focal adhesion and actin filament. For this, we examined the effects of $VEGF_{165}$ or vitronectin or both on the actin filament network and focal

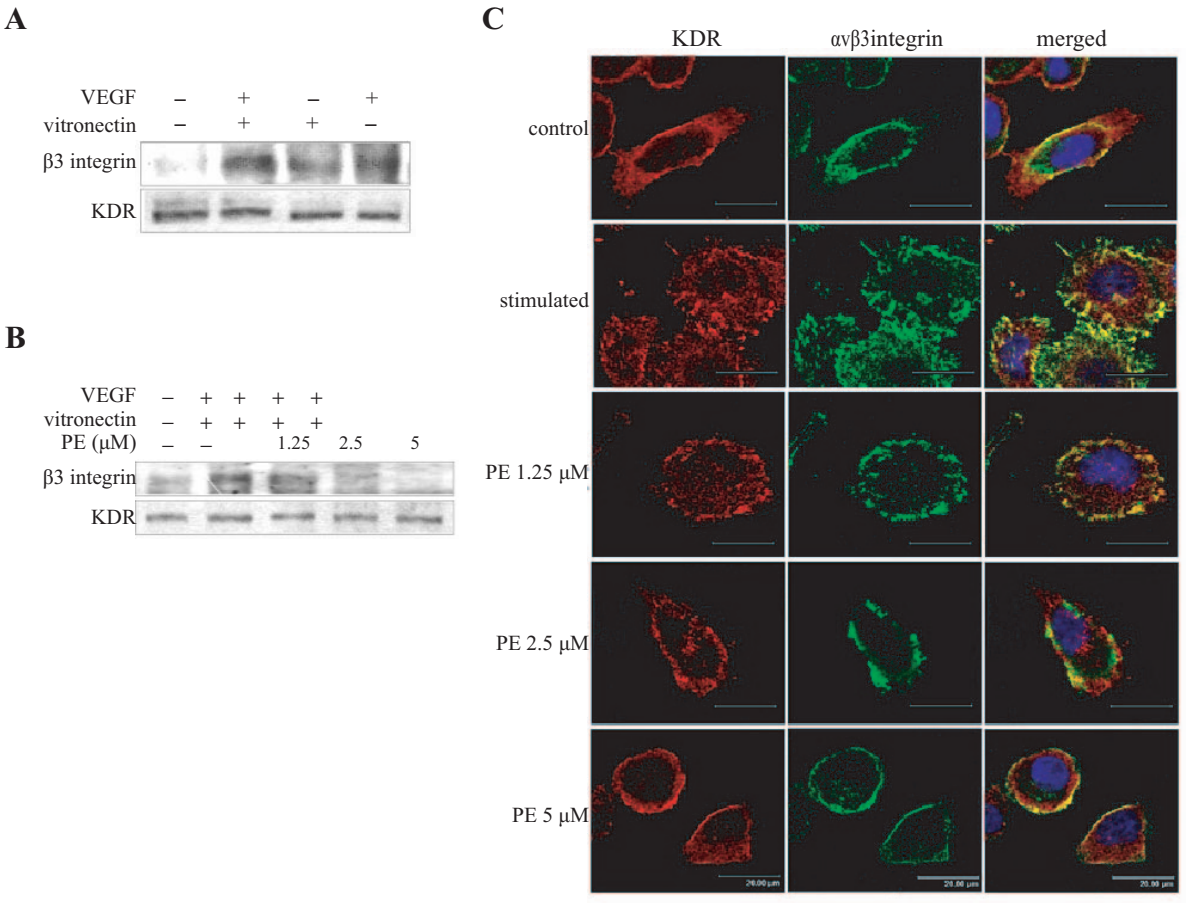

Fig. 3. PE counteracts the association between KDR and $\alpha_v\beta_3$ integrin in HMECs. A, starved HMECs were stimulated with 50 ng/ml VEGF for 10 min or with starved HMECs planted in vitronectin-coated plates for 1 h (or with additional 50 ng/ml VEGF for 10 min). Cells were lysed, and immunoprecipitates obtained with anti-KDR antibody were separated by SDS-polyacrylamide gel electrophoresis and immunoblotted with anti-β_3 integrin antibody and anti-KDR antibody. B, starved HMECs were seeded in vitronectin-coated plates for 1 h and treated with various concentration of PE for 1 h and then exposed to 50 ng/ml VEGF for another 10 min. The association of KDR and $\alpha_v\beta_3$ integrin was determined as described in A. C, starved HMECs seeded in glass coverslips covered with vitronectin were exposed to 50 ng/ml VEGF and incubated for 2 h and then treated with various concentrations of PE for an additional 1 h. Cells were fixed, permeabilized, and incubated with mouse antibody against $\alpha_v\beta_3$ integrin and rabbit antibody against KDR and then subjected to Alexa Fluor 488-anti-rabbit secondary antibody and Alexa Fluor 633-anti-mouse secondary antibody. The fluorescent staining was detected by Leica confocal laser scanning microscope. Representative photograph (magnification, 100×; Scale bars, 20 μm) of three independent experiments with similar results is displayed at right.

adhesion. We found that nonstimulated HMECs were not spread well, with filamentous actin characteristically organized in cortical arrays and vinculin diffused in the perinuclear region (Fig. 5A). Consistently (Avraham et al., 2003; Butler et al., 2003), VEGF- or vitronectin-treated HMECs displayed an increment in actin filament and, in particular, the number of transverse filament bundles that crossed the cell. A noted increase in vinculin immunostaining of focal adhesion occurred at periphery of cells and aligned at the end of actin filament bundles. Furthermore, the stress fiber formation and focal adhesion complex formation induced by vitronectin were significantly enhanced by combination with VEGF, favoring a synergistic effect of VEGF toward vitronectin. PE, however, effectively and dose-dependently suppressed the downstream effects in stress fiber and focal adhesion complex (Fig. 5B), which was, at least to a great extent, a combinatorial result of the simultaneous blockage of PE on both VEGF-KDR interaction and KDR-$\alpha_v\beta_3$ integrin association and thus subsequent signaling transduction.

Because Rac, PAK1, and LIMK1 are the key regulators of the actin dynamics and cell morphology, the effect of PE on the activation of Rac, PAK1, and LIMK1 were also studied. As shown in Fig. 5, C and D, either $VEGF_{165}$ alone or vitronectin alone or the concomitant presence of both induced the activation of Rac, PAK1, and LIMK1, which were markedly reversed by treatment with PE.

We further examined the effect of PE on cell adhesion to vitronectin. Results demonstrated that PE significantly blocked HMEC adhesion to vitronectin (Fig. 5E). This cellular biological function is in fact the combinatorial result of PE on focal adhesion formation and cytoskeleton reorganization and modulation of their main regulators involved.

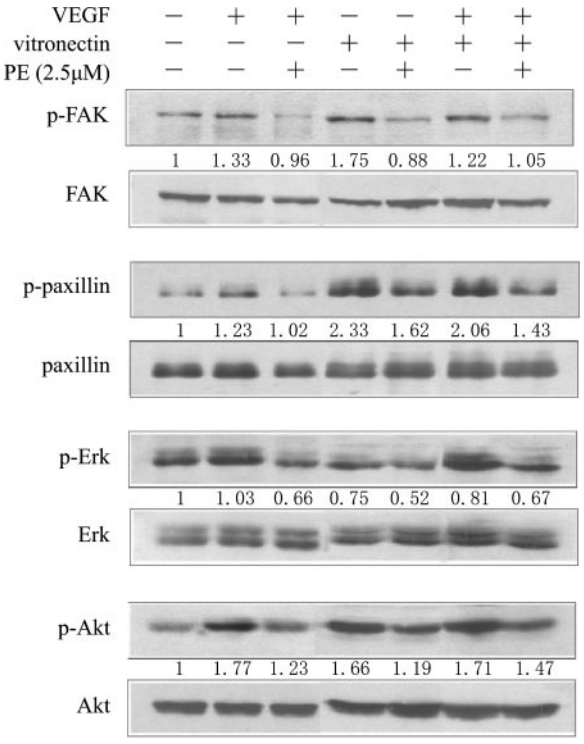

Fig. 4. PE inactivates downstream signaling stimulated by $VEGF_{165}$ and vitronectin in HMECs. Twenty-four-hour-starved HMECs were pretreated with 2.5 μM PE for 1 h and then stimulated with 50 ng/ml VEGF for another 10 min, or starved HMECs were seeded in vitronectin-coated plates for 1 h and then treated with 2.5 μM PE for an additional 1 h. The activation of FAK, paxillin, ERK, and Akt were determined by Western blotting using antibodies against their phosphorylation forms. The membranes were stripped and reprobed with antibodies against FAK, paxillin, ERK, and Akt. Data shown are typical of three independent experiments with similar results. Each protein's phosphorylation level was normalized against its total level.

Discussion

As one of the hallmarks of cancer, angiogenesis is related to tumor development and patient survival. Continuous and intensive research efforts on receptor tyrosine kinases since the 1950s have led to important insight into their molecular mechanism of function and naturally shed light on antiangiogenic therapy by using inhibitors targeting growth factors and their tyrosine kinase receptors. Unlike growth factors such as VEGF targeted by monoclonal neutralizing antibodies, RTKs are often targeted by small chemical compounds to inhibit tyrosine kinase activity. However, with the expanded clinical availability of these compounds, drugs targeting RTKs have met intractable obstacles in cancer treatment, which are probably caused by increasing redundancy of compensatory pathways of angiogenic factors as a tumor progresses or the tumor vasculature matures (Jubb et al., 2006).

Current understanding underscores the cooperative signaling between integrins and RTKs in tumor angiogenesis and development (Eliceiri, 2001). Integrins and RTKs regulate the protein expression of each other (Kim et al., 2000; De et al., 2005). They can directly associate together, thereby modulating the capacity of integrin-RTK complexes and propagating downstream signaling. In fact, the synergistic signaling amplified by integrins and RTKs is increasingly recognized to be essential for tumor migration, invasion, and tumor growth (Orecchia et al., 2003; Cascone et al., 2005; Bon et al., 2006). Taking what we have learned from this point of view, targeting dual signaling pathways cooperated by interaction between integrins and RTKs will reasonably benefit cancer treatment more than the individually targeted event.

In the present study, we proved that PE antagonizes the process of angiogenesis in its distinct mechanism. It interacts with the extracellular domain of KDR, which stands in contrast to the conventional small-molecule inhibitors that rationally interact with the cytoplasmic kinase domain. The most interesting events upon PE's binding to the KDR extracellular domain were to cause the suppression of KDR autophosphorylation and downstream signaling activation on one hand, and to block integrin-mediated pathway upon the abolishment of the physical interaction between KDR and $\alpha_v\beta_3$ integrin on the other hand. All of these will favor in principle the appreciable action of PE in combating against angiogenesis and tumor development.

The next issue challenging us was how PE enabled the disruption of the interaction between KDR and $\alpha_v\beta_3$ integrin upon its association with the extracellular domain of KDR. Physiologically, $\alpha_v\beta_3$ integrin interacts with KDR through its β_3 extracellular region. This might permit the intrinsic engagement of PE with extracellular domain of KDR to competitively inhibit the interaction of KDR with β_3 subunit either via a conformation-based steric hindrance or a share of a common binding site with β_3 integrin. However, the detailed mechanisms deserve our further elucidation. The subsequent inactivation of PE on vitronectin-stimulated

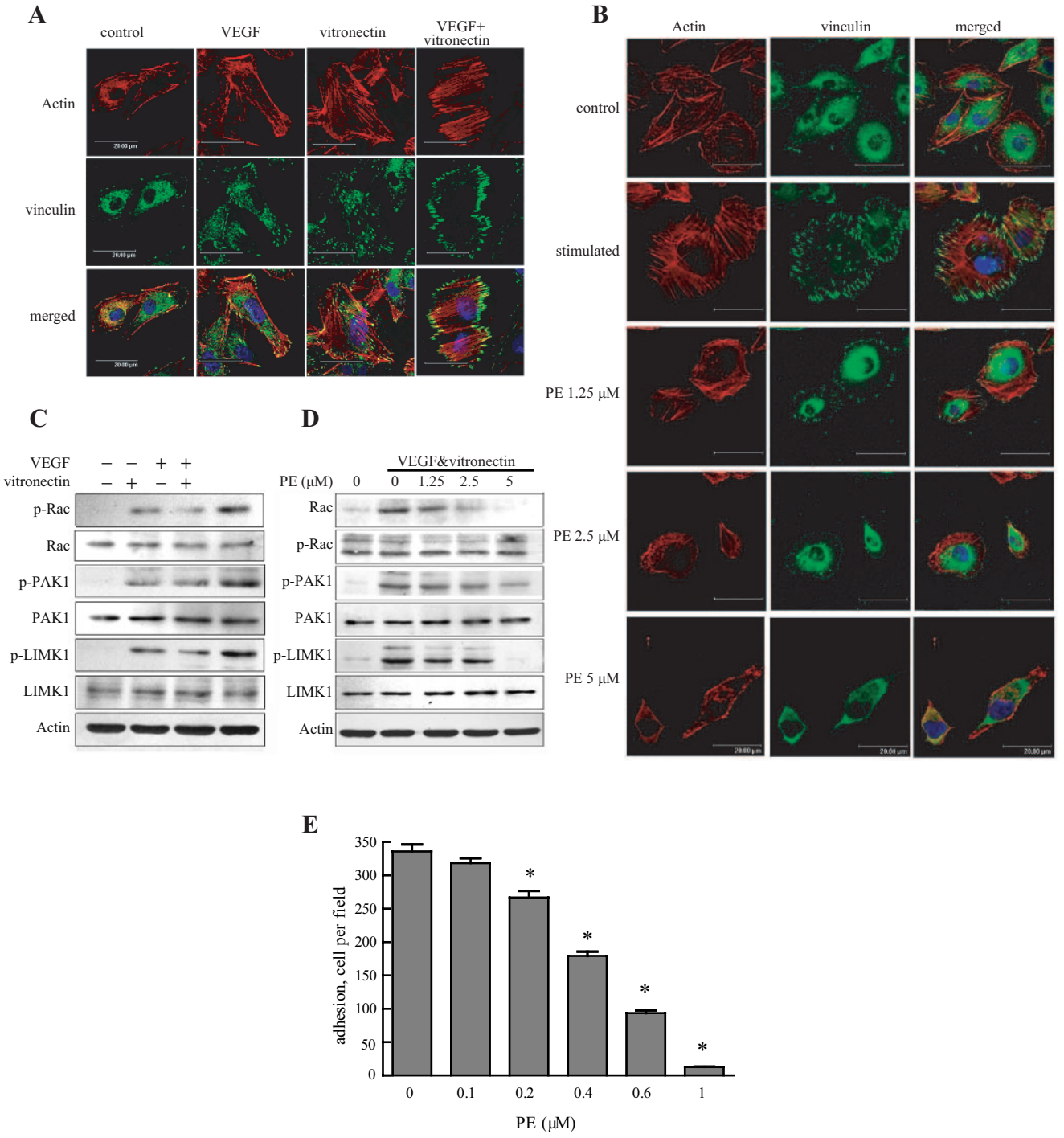

Fig. 5. PE disassembles focal adhesion and actin cytoskeleton; dephosphorylates Rac, PAK1, and LIMK1 in HMECs; and reduces cell adhesion. A, starved HMECs cultured on glass coverslips were stimulated with 20 ng/ml VEGF for 2 h, or starved HMECs plated in glass coverslips were covered with vitronectin for 2 h (or with additional 20 ng/ml VEGF). Cells were fixed, permeabilized, and incubated with mouse antibody against vinculin (stained for focal adhesion) and then followed by incubation of Alexa Fluor 488-anti-mouse secondary antibody, and filamentous actin was stained with Alexa Fluor 532-phalloidin. The fluorescent staining was detected by Leica confocal laser scanning microscope. Representative photograph (magnification, 100×; Scale bars, 20 μm) of three independent experiments with similar results is displayed at top, left. B, starved HMECs were plated on vitronectin-covered glass coverslips and then exposed to 50 ng/ml VEGF. Two hours later, cells were treated with various concentrations of PE for an additional 1 h. Focal adhesion and actin cytoskeleton were detected as described in A. Representative photograph (magnification, 100×; Scale bars, 20 μm) of three independent experiments with similar results is displayed at the top, right. C, starved HMECs were stimulated with 50 ng/ml VEGF for 10 min, or starved HMECs were plated in plates covered with vitronectin for 1 h (or with additional 50 ng/ml VEGF for 10 min). Activation of Rac, PAK1, and LIMK1 was determined by Western blotting using antibodies raised against their phosphorylation forms. The membrane was stripped and reprobed with antibodies against Rac, PAK1, and LIMK1, respectively. D, starved HMECs were seeded in plates covered with vitronectin for 1 h and treated with various concentration of PE for 1 h, followed by the addition of 50 ng/ml VEGF for another 10 min. Activation of Rac, PAK1, and LIMK1 was determined as described in C. E, HMECs were plated on vitronectin-precoated wells for 30 min in a serum-free medium containing the indicated concentrations of PE. Cells were then washed with PBS and counted by 4′,6-diamidino-2-phenylindole staining using an ArrayScan 4.0 HCS Reader (Cellomics). Results (mean ± S.D.) of one experiment (performed in triplicate) representative of three independent experiments are shown. $*$, $P < 0.05$ versus control.

phosphorylation of FAK and paxillin, together with the disassembly of focal adhesion and reorganization of actin cytoskeleton, are thus a combinatorial reflection of the above events, which collectively accounted for its in vitro arrest of HMEC adhesion to vitronectin. One should note that PE markedly inhibits VEGF-driven downstream signaling of $\alpha_v\beta_3$ integrin and related cytoskeleton remodeling. One should also note that there exist synergistic effects of KDR/integrin on focal adhesion-associated remodeling in cytoskeletal structures and appreciably high expression of KDR in endothelial cells. These together help to clarify the preferential nature of PE in targeting endothelial cells and disrupting the focal adhesion and actin stress fibers formation, which in turn promise its distinct inhibitory impact in endothelial cell adhesion, migration, and tumor angiogenesis.

The power of gene-based cancer therapy has been demonstrated by the impressive clinical results obtained with drugs targeting receptor tyrosine kinases. Inspired by the success of Gleevec and intensified by the advent of sorafenib and then sunitinib (Tabernero, 2007), the impetus for developing highly potent drugs of the same kind grows even stronger. Much effort concentrates on developing small chemical compounds targeting the kinase domain of RTKs. Current ongoing evaluation of PE is only the beginning of addressing the scope of its therapeutic potential in cancer therapy. The blockage of physical interaction by integrin-RTK via targeting extracellular domain might thus emerge as an alternative strategy. Borges et al. (2000) have wisely predicted that compounds with potential to disrupt integrin-RTK interaction could be valuable in preventing angiogenesis in tumors, and our work substantiates this notion. With researchers continuing to focus on the structure-based antitumor machineries of PE in particular, it can be hoped that the future will bring a surge of novel innovative, effective inhibitors based on the disruption of integrin-RTK interaction and particularly their cooperative downstream pathways. There is every reason to believe that targeting the dual pathways cooperated by $\alpha_v\beta_3$ integrin-KDR interaction in particular and integrin-RTK in general will harbor greater promise in cancer therapy than in the individual. In addition, the achievable specificity of PE toward KDR stands quite distinct from its derivative philinopside A, which was reported to function as a broad-spectrum RTK inhibitor. This selectivity probably results from the difference in their structures. PE is featured bearing a carbonyl group in C-16, whereas philinopside A instead has an acetoxy group (Tong et al., 2005). Additional work on the structure-activity relationship of this class is currently underway, in the hope that further work will help elucidate the nature behind it.

References

Avraham HK, Lee TH, Koh Y, Kim TA, Jiang S, Sussman M, Samarel AM, and Avraham S (2003) Vascular endothelial growth factor regulates focal adhesion assembly in human brain microvascular endothelial cells through activation of the focal adhesion kinase and related adhesion focal tyrosine kinase. *J Biol Chem* **278:**36661–36668.

Bon G, Folgiero V, Bossi G, Felicioni L, Marchetti A, Sacchi A, and Falcioni R (2006) Loss of beta4 integrin subunit reduces the tumorigenicity of MCF7 mammary cells and causes apoptosis upon hormone deprivation. *Clin Cancer Res* **12:**3280–3287.

Borges E, Jan Y, and Ruoslahti E (2000) Platelet-derived growth factor receptor beta and vascular endothelial growth factor receptor 2 bind to the beta 3 integrin through its extracellular domain. *J Biol Chem* **275:**39867–39873.

Butler B, Williams MP, and Blystone SD (2003) Ligand-dependent activation of integrin $\alpha v\beta 3$. *J Biol Chem* **278:**5264–5270.

Byzova TV, Goldman CK, Pampori N, Thomas KA, Bett A, Shattil SJ, and Plow EF (2000) A mechanism for modulation of cellular responses to VEGF: activation of the integrins. *Mol Cell* **6:**851–860.

Casanovas O, Hicklin DJ, Bergers G, and Hanahan D (2005) Drug resistance by evasion of antiangiogenic targeting of VEGF signaling in late-stage pancreatic islet tumors. *Cancer Cell* **8:**299–309.

Cascone I, Napione L, Maniero F, Serini G, and Bussolino F (2005) Stable interaction between alpha5beta1 integrin and Tie2 tyrosine kinase receptor regulates endothelial cell response to Ang-1. *J Cell Biol* **170:**993–1004.

De S, Razorenova O, McCabe NP, O'Toole T, Qin J, and Byzova TV (2005) VEGF-integrin interplay controls tumor growth and vascularization. *Proc Natl Acad Sci U S A* **102:**7589–7594.

Ek ET, Dass CR, and Choong PF (2006) Pigment epithelium-derived factor: a multimodal tumor inhibitor. *Mol Cancer Ther* **5:**1641–1646.

Eliceiri BP (2001) Integrin and growth factor receptor crosstalk. *Circ Res* **89:**1104–1110.

Holmqvist K, Cross MJ, Rolny C, Hagerkvist R, Rahimi N, Matsumoto T, Claesson-Welsh L, and Welsh M (2004) The adaptor protein Shb binds to tyrosine 1175 in vascular endothelial growth factor (VEGF) receptor-2 and regulates VEGF-dependent cellular migration. *J Biol Chem* **279:**22267–22275.

Jubb AM, Holden S, and Koeppen H (2006) Predicting benefit from antiangiogenic agents in malignancy. *Nat Rev Cancer* **6:**626–635.

Kerbel RS (2005) Therapeutic implications of intrinsic or induced angiogenic growth factor redundancy in tumors revealed. *Cancer Cell* **8:**269–271.

Kim S, Bell K, Mousa SA, and Varner JA (2000) Regulation of angiogenesis in vivo by ligation of integrin alpha5beta1 with the central cell-binding domain of fibronectin. *Am J Pathol* **156:**1345–1362.

Krause DS and Van Etten RA (2005) Tyrosine kinases as targets for cancer therapy. *N Engl J Med* **353:**172–187.

Millauer B, Shawver LK, Plate KH, Risau W, and Ullrich A (1994) Glioblastoma growth inhibited in vivo by a dominant-negative Flk-1 mutant. *Nature* **367:**576–579.

Mitra SK, Hanson DA, and Schlaepfer DD (2005) Focal adhesion kinase: in command and control of cell motility. *Nat Rev Mol Cell Biol* **6:**56–68.

Olsson AK, Dimberg A, Kreuger J, and Claesson-Welsh L (2006) VEGF receptor signalling—in control of vascular function. *Nat Rev Mol Cell Biol* **7:**359–371.

Orecchia A, Lacal PM, Schietroma C, Morea V, Zambruno G, and Failla CM (2003) Vascular endothelial growth factor receptor-1 is deposited in the extracellular matrix by endothelial cells and is a ligand for the alpha 5 beta 1 integrin. *J Cell Sci* **116:**3479–3489.

Saleh M, Stacker SA, and Wilks AF (1996) Inhibition of growth of C6 glioma cells in vivo by expression of antisense vascular endothelial growth factor sequence. *Cancer Res* **56:**393–401.

Shibuya M and Claesson-Welsh L (2006) Signal transduction by VEGF receptors in regulation of angiogenesis and lymphangiogenesis. *Exp Cell Res* **312:**549–560.

Soldi R, Mitola S, Strasly M, Defilippi P, Tarone G, and Bussolino F (1999) Role of alphavbeta3 integrin in the activation of vascular endothelial growth factor receptor-2. *EMBO J* **18:**882–892.

Tabernero J (2007) The role of VEGF and EGFR inhibition: implications for combining anti-VEGF and anti-EGFR agents. *Mol Cancer Res* **5:**203–220.

Tian F, Zhang X, Tong Y, Yi Y, Zhang S, Li L, Sun P, Lin L, and Ding J (2005) PE, a new sulfated saponin from sea cucumber, exhibits anti-angiogenic and anti-tumor activities in vitro and in vivo. *Cancer Biol Ther* **4:**874–882.

Tong Y, Zhang X, Tian F, Yi Y, Xu Q, Li L, Tong L, Lin L, and Ding J (2005) Philinopside A, a novel marine-derived compound possessing dual anti-angiogenic and anti-tumor effects. *Int J Cancer* **114:**843–853.

Zhong L, Guo XN, Zhang XH, Wu ZX, Luo XM, Jiang HL, Lin LP, Zhang XW, and Ding J (2005) Expression and purification of the catalytic domain of human vascular endothelial growth factor receptor 2 for inhibitor screening. *Biochim Biophys Acta* **1722:**254–261.

Address correspondence to: Dr. Jian Ding, Division of Antitumor Pharmacology, State Key Laboratory of Drug Research, Shanghai Institute of *Materia Medica*, Chinese Academy of Sciences, Shanghai, 201203, P.R. China. E-mail: jding@mail.shcnc.ac.cn